Effect of ultrasound-assisted freezing on the physico-chemical properties and volatile compounds of red radish

Bao-guo Xu, Min Zhang, Bhesh Bhandari, Xin-feng Cheng, Md. Nahidul Islam

PII: S1350-4177(15)00105-4
DOI: http://dx.doi.org/10.1016/j.ultsonch.2015.04.014
Reference: ULTSON 2837

To appear in: *Ultrasonics Sonochemistry*

Received Date: 6 February 2015
Revised Date: 11 April 2015
Accepted Date: 17 April 2015

Please cite this article as: B-g. Xu, M. Zhang, B. Bhandari, X-f. Cheng, d.N. Islam, Effect of ultrasound-assisted freezing on the physico-chemical properties and volatile compounds of red radish, *Ultrasonics Sonochemistry* (2015), doi: http://dx.doi.org/10.1016/j.ultsonch.2015.04.014

Effect of ultrasound-assisted freezing on the physico-chemical properties and volatile compounds of red radish

Bao-guo Xu[a], Min Zhang[a*], Bhesh Bhandari[b], Xin-feng Cheng[a] , Md. Nahidul Islam[a]

[a] State Key Laboratory of Food Science and Technology, Jiangnan University, 214122 Wuxi, Jiangsu, China

[b] School of Agriculture and Food Sciences, The University of Queensland, Brisbane, QLD 4072, Australia

*Corresponding author: Professor Min Zhang, School of Food Science and Technology, Jiangnan University, 214122 Wuxi, Jiangsu Province, China.

E-mail: min@jiangnan.edu.cn Fax: 0086-(0)510-85807976

Abstract

Power ultrasound, which can enhance nucleation rate and crystal growth rate, can also affect the physico-chemical properties of immersion frozen products. In this study, the influence of slow freezing (SF), immersion freezing (IF) and ultrasound-assisted freezing (UAF) on physico-chemical properties and volatile compounds of red radish was investigated. Results showed that ultrasound application significantly improved the freezing rate; the freezing time of ultrasound application at 0.26 W/cm^2 was shorten by 14% and 90%, compared to IF and SF, respectively. UAF products showed significant (p<0.05) reduction in drip loss and phytonutrients (anthocyanins, Vitamin C and phenolics) loss. Compared to SF products, IF and UAF products showed better textural preservation and higher calcium content. The radish tissues exhibited better cellular structures under ultrasonic power intensities of 0.17

and 0.26 W/cm^2 with less cell separation and disruption. Volatile compound data revealed that radish aromatic profile was also affected in the freezing process.

Key words: Ultrasound; Immersion freezing; Radish; Calcium; physico-chemical; Microstructure

1. Introduction

Red radish (*Raphanus sativus* L.) cultivars, belonging to the Brassicaceae family, also known as cruciferous vegetables are cultivated in many countries, especially in China. Radish is considered as highly medicinal and nutritional value and suggested as an alternative treatment for various ailments including hyperlipidemia, coronary heart diseases, cancer and so on [1]. Nevertheless, due to its high water content, its shelf life after harvest is quite short. Freezing is one of the most effective preservation method and widely used in the food industry [2]. It is well known that the rate of freezing largely affects the size and distribution of ice crystal in the frozen tissue of foods. High freezing rate leads to the production of smaller crystals evenly distributing throughout the tissue, resulting in slight damages to the tissue [3-6], while slow freezing rate always leads to the formation of larger ice crystals in the extracellular region, resulting in significant damages to the tissue [7]. Therefore, extensive research of new technologies on controlling of crystal size and reducing the time of water–ice transition needs to be carried out.

In recent years, power ultrasound has attracted considerable interest in food science and technology, since it can be applied to develop gentle but targeted

processes to improve the quality and safety of processed foods [8]. Power ultrasound has been proved to be extremely useful in crystallization process [9]. It can play effective roles in the initiation of nuclei and subsequent crystal growth, leading to fine ice crystals and shortening the time between the onset of crystallization and the complete formation of ice during freezing [10]. This is mainly due to the acoustic cavitation, which consists of the formation, growth and violent collapse of numerous small bubbles and the cavitation bubbles which can serve as nuclei for ice nucleation once reaching the critical nucleus size [11].

Some scientists have reported that power ultrasound is extremely effective in the immersion freezing process for fruits and vegetables. Li and Sun [10]reported that the freezing rate was improved greatly when ultrasound power (15.85 W) was applied for 2 min during immersion freezing of potatoes. Sun and Li [2] investigated the microstructural change of potato tissues and showed that the plant tissue exhibited better cellular structure with less intercellular void and cell disruption under ultrasonic power of 15.85 W during immersion freezing. Delgado et al [12] reported the influence of ultrasound on freezing rate of immersion-frozen apples and indicated that different ultrasound intervals, exposure time and initial temperature of ultrasound application affected the nucleation temperature and freezing rate significantly.

Although the application of the power ultrasound in the immersion freezing for fruits and vegetables has been studied for several years, there are very limited studies being published on the physico-chemical properties and volatile compounds dealing with red radish as a product. The main objectives of the current study are to evaluate

the physico-chemical properties of red radish cylinders such as drip loss, color, texture, microstructure, calcium content, total anthocyanins content, vitamin C, total phenolic content and to assess the volatile compound changes of the radish tissue affected by ultrasound-assisted freezing.

2. Materials and methods

2.1. Raw Materials

Red radishes (Xin Ling Mei cultivar, 94.3% w/w moisture content, wet basis) harvested in October 2013 were provided by a farm (Weifang, Shandong province, China). Red radishes were selected according to internal color (uniform red). They were washed in the tap water, drained and dried with a fan. Then they were cut into red radish cylinders measuring 2.5 cm diameter and 3.0 cm high using a regular steel mold (Fig. 1). The radish cylinders were then kept in a refrigerator at a temperature of 4 °C for 6 h to achieve uniform initial temperature until measurements were taken and used up within 2 days for the experimental work.

2.2. Experimental Apparatus

A laboratory scale ultrasonic bath system with a freezing tank (30 cm × 22 cm × 26 cm) (Ningbo Scientz Biotechnology Co., Ltd., Ningbo, China,) was used for red radish immersion freezing assisted with ultrasound. The ultrasonic equipment with 20 kHz frequency and a 30% (w/v) $CaCl_2$ water solution as the freezing medium was fabricated to meet our specifications with tunable electric power at the range of 0–300 W. A temperature control system contained three K-type thermocouples with a data

logger connected to a PC to measure the temperature of freezing tank and samples and a temperature controller to maintain the constant temperature in the freezing tank.

2.3. Experimental Procedure and Design

Fig.1 presents the experimental design. Treatments included slow freezing (SF) in a chamber without air circulation, immersion freezing (IF) in 30% (w/v) $CaCl_2$ (selected $CaCl_2$ concentration allows a liquid solution at freezing temperature), ultrasound-assisted freezing (UAF) in 30% (w/v) $CaCl_2$. For the freezing process, the temperature was set up to reach an average temperature of −20 °C for all the experimental runs. The prepared radish cylinder samples (100 g for each batch) were removed from the refrigerator and a K-type thermocouple (1.0 mm diameter, accuracy ± 0.1 °C) with a digital thermometer (UT325 thermometer, Uni-Trend Technology Limited, Dongguan, China) was inserted into one of the geometric center of the samples. To avoid fluctuations of velocity at different position in the chamber/tank, the sample with K-type thermocouple was specifically placed at the same fixed chosen location for each experiment. In the UAF trials, the samples were irradiated by ultrasound waves with 20 kHz frequency, 30 s on/30 s off duty cycle, and 0.09, 0.17, 0.26, or 0.37 W/cm^2 power intensities. The calorimetric method was used to determine actual dissipated acoustic power and acoustic intensity, as introduced in our previous research [13]. The ultrasound-assisted freezing under different power intensities (0.09, 0.17, 0.26, or 0.37 W/cm^2) were labeled as UAF-1, UAF-2, UAF-3, UAF-4, respectively. The freezing process finished as soon as the temperature of each sample reached -18 °C.

After freezing, each product was immediately placed into a double high-density polyethylene bag and thawed in a constant temperature and humidity chamber (HWS-080, Shanghai Jinghong laboratory instrument Co., Ltd, Shanghai, China) maintained at 20 ± 0.5 ℃ and 70 ± 5 % RH. Thawing was considered complete when the temperature in the geometric center of the products reached 4 ℃. After thawing was completed, the products inside the polyethylene bag were kept in a 4 ℃ refrigerator for further measurements. Each freezing/thawing experiment was undertaken in triplicate.

2.4 Analytical Methods

2.4.1 Drip loss

Thawing was conducted in a constant temperature and humidity chamber and drip loss was calculated using the method suggested by Goncalves et al [14].

$$\text{Drip loss} = (M_2 - M_1)/M_0 \qquad (1)$$

where M_0 (g) was the mass of the sample before thawing, M_1 (g) was the mass of dry blotting paper, M_2 (g) was the weight of wet blotting paper with exuded liquid.

2.4.2 Color analysis

Fresh and frozen/thawed radish cylinders were analyzed for color. A chromaticity instrument (CR-400, Konica Minolta Sensing Inc., Tokyo, Japan) calibrated using a white standard board (L^*=97.75, a^*=–0.03, b^*=1.32) was used to measure the color of surface in the central position of the products. Determinations were carried out on the surface of the products immediately after thawing. The results were expressed as CIE1976 L^*, a^*, b^* scale, where L^* was the degree of lightness, with

100 being very white and 0 being dark; a^* value represents redness (+) and greenness (-), and b^* measures yellowness (+) and blueness (-). The total color difference (ΔE) was a colorimetric parameter extensively used to characterize the variation of colors in products during processing by applying the following equation:

$$\Delta E = \pm\sqrt{(L_0^* - L^*)^2 + (a_0^* - a^*)^2 + (b_0^* - b^*)^2} \quad (2)$$

where L_0^*, a_0^* and b_0^* were the color readings of fresh samples. The measurements were carried out on 6 different radish cylinders for each batch.

2.4.3 Firmness Analysis

The firmness was measured by using a texture analyzer (TA-XT2 of Stable Micro Systems, Ltd., Surrey, UK) in compression mode with a 2-mm diameter cylindrical probe (SMS-P/2, Stable Micro Systems, Ltd., Surrey, UK). The operating parameters were pretest speed (2.00 mm/s), test speed (1.00 mm/s), sample strain (50 %), posttest speed (5.00 mm/s) and trigger force (5.0 g). The force–deformation curves were recorded using a software provided by the manufacturer, and the maximum force (N) was calculated and used as firmness. Six replicates were carried out.

2.4.4 Analysis of Total Calcium Content

The total calcium content was analysed by an atomic absorption spectrophotometry (AAS) after acid digestion with HNO_3 [15]. About 5 g of radish samples were digested with 2 mL of 65 % HNO_3 solution and put into a muffle furnace at about 550 °C for 4 h. Residues were diluted to a proper concentration for measurement using AAS. Lanthanum solution and HNO_3 was added to reach a final

concentration of 10 % and 2 %, respectively. The solution obtained was used to determine calcium using a flame atomic absorption spectrometer (Spectr AA, Varian, Palo Alto, USA).

2.4.5 Total anthocyanin content

The method of anthocyanin extraction for radish samples was from Jing et al [16] with some modifications. About 10 g of radish slurry samples were transferred to a flask containing 20 ml of acidified acetone (concentrated HCl/70% aqueous acetone = 0.01:100 mL) and mixed thoroughly. All flasks were stirred with the aid of the magnetic stirrer for 20 min. Slurry were filtered through a Shuang-Quan #101 filter paper (Hangzhou Whatman Filter Paper Co., Hangzhou, China) under vacuum using a Büchner funnel. The residues were re-extracted twice with 10 mL of acidified acetone for each extraction. All filtrates were combined and made up to a 100 mL in volumetric flask with acidified acetone. After this period of time, the extracts were immediately analysed.

The total anthocyanin content was determined according to the spectrophotometric pH-differential method [17]. Briefly, 1 mL of the extract was mixed with 0.025 M potassium chloride buffer (pH 1.0, 4 mL) and 0.4 M sodium acetate buffer (pH 4.5, 4 mL), respectively. Absorbance of the mixture was measured at 520 and 700 nm using an UV-Vis spectrophotometer (Model UV2600; Techcomp, Shanghai, China). The total anthocyanin content was calculated using following equation:

$$\text{Tatal anthocyanin content (mg/L)} = A \times MW \times DF \times 1000/\varepsilon \times 1 \quad (3)$$

Where *A* (absorbance) = $(A_{510}\text{-}A_{700})_{PH\ 1.0}$ - $(A_{510}\text{-}A_{700})_{PH\ 4.5}$; MW (molecular weight) = 433.2 g/mol and ε (molar absorptivity coefficient) = 31,600 L/mol/cm for pelargonidin-3-glucoside (P3G) of red radish [16], DF = dilution factor; 1000 = conversion from g to mg; 1 = path length in cm. The total anthocyanin content was then expressed as mg P3G/100 g of fresh weigh by dividing it with solid to solvent ratio 0.1 g/mL. Analysis for each treatment was performed in triplicate.

2.4.6 Vitamin C

Ascorbic acid content was determined using standard 2,6-dichloro-indophenol titration method [18]. Data were calculated on a fresh weight and expressed as mg/100 g FW. The analysis was done in triplicate and the averages of these measurements were reported.

2.4.7 Total phenolic content

The amount of total phenolic was determined using Folin–Ciocalteu (FC) method [19] with some modifications. About 1 g raw and homogenized samples were extracted with 15% aqueous ethanol (10 mL) on a mechanical shaker for 1 h in the 30 °C water bath. The mixture was centrifuged at 9,500 rpm for 15 min and the supernatant decanted into polypropylene tubes. Supernatants were filtered through Shuang-Quan #102 filter paper.

Briefly, 1 mL of extract was mixed thoroughly with 95% aqueous ethanol (15 mL), distilled water (60 mL) and Folin–Ciocalteu reagent (3 mL). After shaking for 3 min, 10 mL of 16.7 % Na_2CO_3 was added into the reaction mixture and then made up to a 100 mL in volumetric flask with distilled water. Finally the reaction mixture was

kept for 60 min in the dark before measuring its absorbance in a single beam UV–vis spectrophotometer (Model UV2600; Techcomp, Shanghai, China) at 765 nm [20]. A calibration curve was performed for standard gallic acid (R^2 = 0.999, y = 0.0012x − 0.0074) and the results were expressed as milligram of gallic acid equivalents/100 g fresh weight, i.e. mg GAE/100 g FW. Analysis for each treatment was performed in triplicate.

2.4.8 Light microscopic analysis

The samples (Fresh, SF, IF and UAF) were prepared on slices by cutting fibers longitudinally using razor blade into slices less than 15 μm thick then stored at 4 °C until used. Microstructures of samples were analyzed under a light microscope (Model: Olympus BX43, Tokyo, Japan) equipped with a digital camera (Smart V350D, Jiangsu JEDA Science-Technology Development Co., LTD, China). Micrographs were taken at 200 times magnification. All the microstructure examinations and micrographs were performed at the ambient temperature 20 ± 2 °C.

2.4.9 Volatile compound (SPME-GC-MS) analysis

The volatile compounds of fresh and thawed radish were investigated by headspace solid-space microextraction (HS-SPME) combined with gas chromatography–mass spectrometry. 5 g of minced radish samples was weighed into a 15 mL headspace vial and sealed with a PTFE-faced silicone septum. A SPME device containing a fused-silica fibre (Supelco, USA) coated with a 75 μm layer of CAR/PDMS (Carboxen/Polydimethylsiloxane) was used. Then, a SPME fibre was exposed to the headspace while maintaining the sample at 50 °C for 30 min. The fibre

with compounds was retracted back into the needle and transferred to the injection port of gas chromatograph immediately. A time period of 3 min was adopted for desorption and conditioning at the desorption temperature of 250 °C.

The GC-MS were performed using a gas chromatography mass spectrophotometer (GC 6890/MS 5975, Agilent, USA). The compounds were separated using a DB-WAX capillary column (30.0 m 250 μm I.D., 0.25 μm film thickness, Supelco, USA). The sample was injected in splitless mode. Helium was used as a carrier gas with a velocity of 0.8 mL/min. The temperature programme was isothermal for 3 min at 40 °C, raised to 90 °C at a rate of 5 °C/min, then raised to 230 °C at a rate of 10 °C/min, and held for 7 min: total run time is 34 min. Injector and detector temperatures were both set at 250 °C. The mass spectra were obtained using a mass selective detector working in ionization mode of EI+, emission current of 80 μA, electron energy of 70 eV, scanning mass range of 33–450 m/z and detector voltage of 1000 V. The interface and source temperature were 250 and 200 °C, respectively.

The identity of the odorants was determined by a comparison of the Kovats index (KI) of a series of n-alkane (C7–C21) with the mass spectra library of NIST98 (National Institute of Standards of Technology, Hewlett–Packard, MD, USA). The integration reports were accepted if matching degree was above 800. The relative contents of flavor compounds were determined by comparing the percentage of peak areas.

2.5. Statistical Analysis

Statistical analysis of variance (ANOVA) was performed using SPSS 20.0 software (IBM, Chicago, IL, USA). The significant difference between two means was determined by using Tukey's test procedure at 95 % confidence level (p<0.05).

3. Results and Discussion

3.1 Effect of different freezing conditions on the freezing time

Rapidly freezing produces small intracellular ice, while slowly freezing produces large ice crystals. Thus minimising the time of freezing can contribute to better retention of the final quality of frozen product [12, 21]. Many factors affect the freezing time, including temperature difference between freezing medium and food, effective heat transfer coefficient, product shape/size, and physical properties of the food. The freezing curves of radish cylinders during the process of SF, IF and UAF at different power intensities are depicted in Fig. 2. The trend of those six freezing curves was similar. All of them included three stages: a liquid-state temperature decrease stage (>0 °C), a phase transition stage (0 to -5 °C) and a solid-state temperature decrease stage (<-5 °C). However, remarkable difference on the freezing time between SF and IF/UAF was observed. The freezing time of SF was the highest, which was nearly 8 times higher than that of IF and UAF. This showed that the freezing time was greatly shortened under IF and UAF conditions.

The freezing time of UAF-3 was the lowest, followed by UAF-1, UAF-2, UAF-4, while IF was the highest. It implied that different ultrasound power intensities resulted in different freezing times. The freezing times of UAF were lower than that of IF. This was due to significant heat transfer enhancement [22] and the plenty of cavitation

266 bubbles formation [8] by ultrasound application during freezing process.

267 Three effects, inducing nucleation, heat transfer enhancement, and heat
268 generation (thermal effect), were caused by the propagation of ultrasonic waves into
269 the samples [23]. Nucleation and heat transfer enhancement would shorten the
270 freezing time, while the effect of heat generation was adverse to it. In addition, the
271 higher the power was delivered, the higher the intensity of agitation was produced,
272 thus resulting in higher heat transfer enhancement. Therefore, with the increasing of
273 ultrasound irradiation power intensities, the rate of heat transfer improved. That was
274 why the total freezing time of UAF-2 (744 s) was shorter than UAF-1 (792 s), but
275 longer than UAF-3 (722 s). However, the total freezing time of the highest power
276 intensity UAF-4 was the longest (806 s). This might be attributed to the fact that heat
277 produced by ultrasound cannot be neglected in freezing process. More acoustic energy
278 is converted into heat and absorbed by the medium when more ultrasonic wave is
279 delivered to the medium [10]. Similar results were reported by Hu et al [23] and Li
280 and Sun [10] who also got the similar trends on the material of dough and potatoes,
281 respectively.

282 ***3.2 Effect of different freezing conditions on the thawing time and drip loss***

283 Frozen radish cylinders with different freezing processes were thawed under the
284 same temperature, humidity and position in the chamber. The thawing times of the
285 frozen radish cylinders presented in Fig. 3 were different. The thawing time of SF
286 products was longest (77 min), followed by IF (65 min), while under applying
287 ultrasound irradiation of 0.09, 0.17, 0.26, or 0.37 W/cm^2, thawing times were 52, 48,

49 and 54 min, respectively. As the trend shows, the ultrasound irradiation was an effective process to reduce the thawing time. This might be due to the fact that the shorter freezing time resulted in smaller ice crystals inside the radish tissues, leading to less thawing time of frozen radish products.

From Fig. 2 and Fig. 3, it can be concluded that drip loss strongly depended on freezing time. As expected, SF had higher value of drip loss than that of IF and UAF. Compared to SF products, 35% and 53% reduction in the drip loss were achieved for IF and UAF-2, respectively. This was probably due to the formation of larger ice crystals in the extracellular space of SF, leading to more separation and disruption of cells. In contrast, quick-freezing causes less cell wall damage, since only small ice crystals are formed intracellularly [24, 25]. In addition, the presence of calcium (Table 1) in the solution for IF and UAF, contributed to maintaining the cell-wall structure by interacting with the pectic acid in the cell walls to form calcium pectate, may also play a role in the reduction of the drip loss [26]. Slight difference in drip loss between UAF-2 and UAF-3 products was also observed from Fig. 3. Compared to IF, UAF-1 and UAF-4 products, UAF-2 products provided remarkable decrease in drip loss. This was probably due to faster primary nucleation, the production of smaller crystals with better size uniformity and reduction of cell damage by sonocrystallization under proper power intensity.

3.3 Effect of different freezing conditions on the color

Fig.4 shows the chromatic change of the surface of radish cylinders subjected to SF, IF and different UAF processes. Compared to the fresh samples, L^*, a^* and b^*

values of the products with different freezing processes were all decreased. Analyzing the L^* values, no significant differences ($p>0.05$) were found among those products frozen by immersion freezing with/without ultrasound irradiation. However, compared to products of SF, products of IF and UAF exhibited significantly higher L^* values. After thawing, a^* values of SF products was significantly lower than that of IF and UAF products, which might be the result of bigger crystal formation, more disrupted cell walls and drip loss. No significant differences ($p>0.05$) of a^* values of IF and UAF products was observed. The variations of b^* values obtained in this study were slightly decreased. SF process had much stronger impact than IF and UAF on overall color change of radish cylinders by analyzing the values of the total color difference (ΔE). From the results obtained in this study, it implied that slight improvement in the color of radish cylinders was achieved by using ultrasound.

3.4 Effect of different freezing conditions on total calcium content and texture

Calcium processing is popular in the fruits and vegetables industry due to the fact that calcium can not only maintain the shelf life of fresh vegetables and fruits to improve the quality of products, but also can complement the necessary requirements for human body. As can be seen from Table 1, there was no significant ($p>0.05$) difference of total calcium content between fresh radish and SF products. During immersion freezing process, the calcium can be absorbed from the liquid coolant into the product. Table 1 shows that the total calcium content of the immersion frozen samples in $CaCl_2$ solutions significantly ($p<0.05$) increased, compared to that of fresh and SF samples. Additionally, the ultrasonic treatment resulted in significant ($p<0.05$)

increase in total calcium content compared to that in IF products. This is because the mass transfer was increased by the ultrasound application during ultrasound-assisted freezing process.

Texture is a critical quality characteristic in the consumer acceptability of fresh fruit and vegetables. The firmness of SF products was the lowest, which decreased by approximately 72% with respect to fresh samples, followed by IF, UAF-1, UAF-4 and UAF-2, while UAF-3 was the highest (Fig. 5). It implied that the immersion freezing in $CaCl_2$ solution showed remarkable improvement on the texture of products. This is because calcium ions from the freezing coolant to the samples formed cross-links or bridges between free carboxyl groups of the pectin chains, resulting in strengthening of the cell wall [27]. In addition, significant difference (p<0.05) was observed between the IF and UAF, which might be due to the fact that lower freezing rate caused severe changes in product microstructure (more large intercellular spaces and strong cell collapse).

3.5 Effect of different freezing conditions on the nutritional value

Anthocyanins are plant pigments responsible for the orange, red, and blue colors of several fruits and vegetables. The stability of anthocyanin is influenced by pH, light, oxygen, enzymes and temperature during processing [28, 29]. As can been seen from the Table 1, total anthocyanin contents of radish cylinders with different freezing processes were lower than fresh ones, especially for the SF products, which showed 26% reduction. In theory, degradation of anthocyanin may happen during ultrasound application as free radicals generated due to cavitation can attack

anthocyanins [21]. However, significant improvement of the total anthocyanin retention was obtained by using the UAF compared to IF and SF. This was attributed to the fact that the drip loss of UAF were lower than that of IF and SF; and the effect of drip loss to the anthocyanin loss was greater than that of anthocyanin degradation resulting from cavitation by ultrasound irradiation.

Vitamin C content is a critical criterion in determining the quality of fruits and vegetables. There was a decrease in vitamin C content of radish cylinders after freezing/thawing (Table 1). Theoretically, the degradation of vitamin C during ultrasound application is caused by either thermolysis, combustion occurring inside the bubble or by reaction with hydroxyl radicals [21]. However, significantly (p<0.05) higher retention of vitamin C in UAF products was observed compared to SF and IF products. As mentioned above (Fig. 3), significant differences (p<0.05) of drip loss were observed between UAF and SF/IF products. This might be justified with the fact that the effect of drip loss on vitamin C loss was higher than degradation by ultrasound irradiation. In addition, the retention of vitamin C of UAF-4 products was the lowest, and there were no significant difference (p>0.05) among UAF-1, UAF-2 and UAF-3 products.

Total phenolic content of radish cylinders after freezing/thawing are also shown in Table 1. Significant difference (p<0.05) was observed between the fresh samples and the products with different freezing processes, while there were no significant difference (p>0.05) among UAF products at various power intensities. The highest retention of total phenolic content was UAF-3 (83.06 mg GAE/100 g FW), while the

lowest was SF (71.21 mg GAE/100 g FW). Previous works had reported that phenol and its chloro/nitro derivatives are largely soluble in water so that the main reaction site for their destruction during ultrasonic irradiation was the bulk liquid, where the attack of hydroxyl radicals on the ring carbons results in various oxidation intermediates [30]. Accordingly, the main reason for the improvement of phenolic content retention under ultrasound-assisted freezing was attributed to the fact that ultrasound irradiation improved the freezing rate and thus the dominating ice crystals in the cell were smaller, resulting in less drip loss.

3.6 Effect of different freezing conditions on the microstructure

Fig. 6 shows the light micrographs of thawed radish tissue under the different freezing conditions. A fresh sample of radish with integrity of parenchymatous tissue and intact membranes can be observed in Fig. 6a. Fig. 6b shows the light micrograph of radish tissue frozen by SF. Cell wall disruption and cell separation were distinctly viewed. These disruption and separation caused an increase of intercellular spaces. In addition, the cells appeared torn and irregular in shape and distortion in tissue were also observed in some regions of SF radish tissue.

Fig. 6c shows that the shapes of cells of IF products were more regular and less torn compared to Fig. 6b. However, many cells were still separated and some cell walls were disrupted. The light micrographs for frozen-then-thawed radish tissues under various ultrasonic power intensities are shown in Figs. 6d-g. It can be seen that there was a considerable difference in the microstructure of radish tissues under the treatments of various ultrasonic power intensities. Under the UAF-2 and UAF-3, the

cells packed tightly with neighbouring ones and little intercellular spaces were observed. No cell wall disruption happened, but few cells separation was observed. It implied that the presence of very small ice crystals inside and outside the cells resulted in the intercellular spaces without enlargement, the plasma membrane still close to the cell wall and the cell walls without rupture. Very similar results were observed between the micrographs of UAF-1 and UAF-4, in which both cell wall disruption and cell separation occurred. This is because insufficient and excessive effects of ultrasound irradiation of 0.09 W and 0.37 W/cm^2 power intensities, can only slightly enhance the freezing rate, leading to the formation of larger ice crystals.

Most foodstuffs consist of animal and/or vegetable cells to form biological tissues. The solution of the tissues is contained between the cells (extracellular fluid) or inside the cell (intracellular fluid). Meanwhile, the concentration of intracellular fluid is higher than that in the extracellular region and freezing usually occurs first in the extracellular region when the sample is frozen [31]. During the process of phase change of water in the extracellular fluid into ice, the intracellular fluid still remains in supercooled condition. Therefore, the vapor pressure of the intracellular fluid will be higher than that of the extracellular fluid and ice crystals. The pressure difference results in the moving of the intracellular water from cells to deposit on the extracellular ice crystals thus the growing of large ice crystals [32]. If the ice crystals are large enough, it can deform the cells, or even rupture the cells permanently. In the current work, Fig. 6b illustrated this effect. When thawed, it would increase the drip loss, decrease the firmness and reduce the overall quality of the food. The data in Fig.

3-5 and Table 1 also can prove this conclusion.

3.7 Effect of different freezing conditions on the volatile compounds

Volatile compounds of fruits and vegetables can be usually affected by freezing. During freezing process, the integrity of cellular compartments can be damaged by the formation of ice crystal and cellular membranes can lose the osmotic status and semi-permeability [33]. In addition, the metabolic system of the plant tissue can be interrupted, the enzymatic systems dislocate and the cell can lose its turgor. Also, bio-chemical deterioration reactions can occur [34].

The total volatile compounds in fresh and frozen-thawed radish samples are shown in Table 2. At the end of process, more than 50 volatile compounds were detected in the radish samples, including alcohols, aldehydes, ketones, esters and sulphurs and other compounds. The major volatiles identified in the present study were sulphur compounds in both fresh and thawed radish samples, which was also reported by Gao et al [35]. The most abundant sulphur compound in the red radish was 4-isothiocyanato-1-(methylthio)-1-Butene. From Table 2, the most heavily affected compound was also 4-isothiocyanato-1-(methylthio)-1-Butene during freezing-thawing process. The relative amount of this compound in the fresh samples was 38.10% of total amount of volatiles (based on the peak area), while it remarkably increased to around 60% in the frozen/thawed radish samples. This is because the odor and taste typical of brassica vegetables are mainly due to glucosinolates (GLS) and their breakdown products such as isothiocyanates, organic cyanides, oxazolidinethiones, and thiocyanate. Cellular structure disruption of brassica

vegetables by freezing results in glucosinolate degradation and formation of several breakdown products [36].

Compared to fresh radish samples, the alcohols, aldehydes, ketones and other compounds content of thawed samples were much lower. From the result, it implied that freezing-thawing process significantly affected the volatile compounds of red radish and the most abundant compound of 4-isothiocyanato-1-(methylthio)-1-Butene in red radish was also the most heavily affected compound.

4. Conclusion

The effects of ultrasound irradiation on the radish-freezing process, as well as the physico-chemical properties and volatile compounds of ultrasound-assisted frozen radish cylinders were investigated. The results showed that UAF provided significant benefit in reducing drip loss as compared to SF. In addition, IF and UAF showed significant benefit for maintaining original firmness and color. Compared to SF and IF, the microstructure of radish cylinders was found better preserved by the application of ultrasound-assisted freezing.

The retention of phytonutrients (anthocyanins, Vitamin C and phenolics) of radish cylinders after freezing/thawing process by UAF was higher than that of IF and SF. The main reasons for this was justified with the fact that ultrasound irradiation improved the freezing rate and thus the domain ice crystals in the cell were smaller, resulting in less drip loss. The retention of phytonutrients after freezing/thawing process strongly depended on drip loss rather than degradation by ultrasound irradiation. The calcium content of IF and UAF products were significantly higher

than that of fresh and SF samples. SPME-GC-MS analysis showed that the volatile compounds of red radish deeply affected .

5. Acknowledgements

The authors thank the financial support from China National Natural Science Foundation (Contract No. 21176104) which has enabled us to carry out this study.

Reference

[1] l.S. Curtis, The noble radish: past, present and future, Trends in Plant Science, 8 (2003) 305-307.

[2] D.-W. Sun, B. Li, Microstructural change of potato tissues frozen by ultrasound-assisted immersion freezing, Journal of food engineering, 57 (2003) 337-345.

[3] S. Ahmad, P. Yaghmaee, T. Durance, Optimization of Dehydration of Lactobacillus salivarius Using Radiant Energy Vacuum, Food and Bioprocess Technology, 5 (2010) 1019-1027.

[4] L.C. Ming, R.A. Rahim, H.Y. Wan, A.B. Ariff, Formulation of Protective Agents for Improvement of Lactobacillus salivarius I 24 Survival Rate Subjected to Freeze Drying for Production of Live Cells in Powderized Form, Food and Bioprocess Technology, 2 (2009) 431-436.

[5] F. Streit, G. Corrieu, C. Béal, Effect of Centrifugation Conditions on the Cryotolerance of Lactobacillus bulgaricus CFL1, Food and Bioprocess Technology, 3 (2008) 36-42.

[6] S. Yu, Y. Ma, X. Zheng, X. Liu, D.-W. Sun, Impacts of Low and Ultra-Low Temperature Freezing on Retrogradation Properties of Rice Amylopectin During Storage, Food and Bioprocess Technology, 5 (2011) 391-400.

[7] L. Zheng, D.-W. Sun, Innovative applications of power ultrasound during food freezing processes—a review, Trends in Food Science & Technology, 17 (2006) 16-23.

[8] D. Knorr, M. Zenker, V. Heinz, D.-U. Lee, Applications and potential of ultrasonics in food processing, Trends in Food Science & Technology, 15 (2004) 261-266.

[9] H. Kiani, Z. Zhang, A. Delgado, D.-W. Sun, Ultrasound assisted nucleation of some liquid and solid model foods during freezing, Food Research International, 44 (2011) 2915-2921.

[10] B. Li, D.-W. Sun, Effect of power ultrasound on freezing rate during immersion freezing of potatoes, Journal of food engineering, 55 (2002) 277-282.

[11] T. Mason, L. Paniwnyk, J. Lorimer, The uses of ultrasound in food technology, Ultrasonics sonochemistry, 3 (1996) S253-S260.

[12] A.E. Delgado, L. Zheng, D.-W. Sun, Influence of Ultrasound on Freezing Rate of

Immersion-frozen Apples, Food and Bioprocess Technology, 2 (2009) 263-270.

[13] B. Xu, M. Zhang, B. Bhandari, X. Cheng, Influence of power ultrasound on ice nucleation of radish cylinders during ultrasound-assisted immersion freezing, International Journal of Refrigeration, 46 (2014) 1-8.

[14] E.M. Gonçalves, M. Abreu, T.R.S. Brandão, C.L.M. Silva, Degradation kinetics of colour, vitamin C and drip loss in frozen broccoli (Brassica oleracea L. ssp. Italica) during storage at isothermal and non-isothermal conditions, International Journal of Refrigeration, 34 (2011) 2136-2144.

[15] L.M. Kawashima, L.M. Valente Soares, Mineral profile of raw and cooked leafy vegetables consumed in Southern Brazil, Journal of Food Composition and Analysis, 16 (2003) 605-611.

[16] P. Jing, S.-J. Zhao, S.-Y. Ruan, Z.-H. Xie, Y. Dong, L. Yu, Anthocyanin and glucosinolate occurrences in the roots of Chinese red radish (Raphanus sativus L.), and their stability to heat and pH, Food Chemistry, 133 (2012) 1569-1576.

[17] J. Lee, R.W. Durst, R.E. Wrolstad, Determination of total monomeric anthocyanin pigment content of fruit juices, beverages, natural colorants, and wines by the pH differential method: Collaborative study, Journal of AOAC international, 88 (2005) 1269-1278.

[18] Z. Min, L. Chunli, D. Xiaolin, Effects of heating conditions on the thermal denaturation of white mushroom suitable for dehydration, Drying technology, 23 (2005) 1119-1125.

[19] C.Y. Cheok, N.L. Chin, Y.A. Yusof, R.A. Talib, C.L. Law, Optimization of total monomeric anthocyanin (TMA) and total phenolic content (TPC) extractions from mangosteen (Garcinia mangostana Linn.) hull using ultrasonic treatments, Industrial Crops and Products, 50 (2013) 1-7.

[20] V. Singleton, J.A. Rossi, Colorimetry of total phenolics with phosphomolybdic-phosphotungstic acid reagents, American journal of Enology and Viticulture, 16 (1965) 144-158.

[21] F.A.N. Fernandes, S. Rodrigues, Ultrasound Applications in Fruit Processing, in: S. Rodrigues, F.A.N. Fernandes, (Eds), Advances in Fruit Processing Technologies. CRC Press, Taylor and Francis Group, LLC, USA, 2012, pp. 51–86.

528 [22] S. Sastry, G. Shen, J. Blaisdell, Effect of Ultrasonic Vibration on Fluid-to-Particle
529 Convective Heat Transfer Coefficients, Journal of Food Science, 54 (1989) 229-230.
530 [23] S.-Q. Hu, G. Liu, L. Li, Z.-X. Li, Y. Hou, An improvement in the immersion freezing
531 process for frozen dough via ultrasound irradiation, Journal of Food Engineering, 114
532 (2013) 22-28.
533 [24] S. Van Buggenhout, D. Sila, T. Duvetter, A. Van Loey, M. Hendrickx, Pectins in
534 processed fruits and vegetables: Part III—Texture engineering, Comprehensive Reviews
535 in Food Science and Food Safety, 8 (2009) 105-117.
536 [25] A.E. Delgado, A.C. Rubiolo, Microstructural changes in strawberry after freezing and
537 thawing processes, LWT - Food Science and Technology, 38 (2005) 135-142.
538 [26] C.D. Galetto, R.A. Verdini, S.E. Zorrilla, A.C. Rubiolo, Freezing of strawberries by
539 immersion in $CaCl_2$ solutions, Food Chemistry, 123 (2010) 243-248.
540 [27] A.B. Martín-Diana, D. Rico, J.M. Frías, J.M. Barat, G.T.M. Henehan, C. Barry-Ryan,
541 Calcium for extending the shelf life of fresh whole and minimally processed fruits and
542 vegetables: a review, Trends in Food Science & Technology, 18 (2007) 210-218.
543 [28] R.L. Jackman, R.Y. Yada, M.A. TUNG, R. Speers, Anthocyanins as food colorants—a
544 review, Journal of Food Biochemistry, 11 (1987) 201-247.
545 [29] W.-D. Wang, S.-Y. Xu, Degradation kinetics of anthocyanins in blackberry juice and
546 concentrate, Journal of Food Engineering, 82 (2007) 271-275.
547 [30] R. Kidak, N.H. Ince, Ultrasonic destruction of phenol and substituted phenols: a review
548 of current research, Ultrasonics sonochemistry, 13 (2006) 195-199.
549 [31] Fennema O., Nature of the freezing process, in: R.O. Fennema, D.W. Powrie, E.H. Marth
550 (Eds), Low temperature preservation of food and living matter. Marcel Dekker Inc., New
551 York, 1973, pp. 151–227.
552 [32] M.E. Sahagian, H.D. Goff, Fundamental aspects of the freezing process, in: L.E.Jeremiah,
553 (Ed), Freezing Effects on Food Quality. Marcel Dekker. New York, 1996, pp. 1–50.
554 [33] N.B. Tregunno, H.D. Goff, Osmodehydrofreezing of apples: structural and textural
555 effects, Food Research International, 29 (1996) 471-479.
556 [34] P. Talens, I. Escriche, N. Martínez-Navarrete, A. Chiralt, Influence of osmotic
557 dehydration and freezing on the volatile profile of kiwi fruit, Food Research International,

558 36 (2003) 635-642.
559 [35] R. Gao, P. Jing, S. Ruan, Y. Zhang, S. Zhao, Z. Cai, B. Qian, Removal of off-flavours
560 from radish (Raphanus sativus L.) anthocyanin-rich pigments using chitosan and its
561 mechanism(s), Food Chemistry, 146 (2014) 423-428.
562 [36] I. Blažević, J. Mastelić, Glucosinolate degradation products and other bound and free
563 volatiles in the leaves and roots of radish (Raphanus sativus L.), Food Chemistry, 113
564 (2009) 96-102.
565
566

Figure captions

Fig.1 Flowchart for experimental design; SF: slow freezing, IF: immersion freezing in 30% (w/v) $CaCl_2$, UAF: ultrasound-assisted freezing in 30% (w/v) $CaCl_2$.

Fig.2 The freezing curves of radish cylinders during the process of SF, IF and UAF at different power intensities. (n=5).

Fig.3 The thawing time and drip loss of radish cylinders frozen by SF, IF, and UAF at different power intensities. (n=3); different lowercase superscript letters (a–d) represent significant differences of thawing time (p<0.05); different capital subscript letters (A–D) represent significant differences of drip loss (p<0.05).

Fig.4 The color of fresh and thawed radish cylinders. (n=6); different lowercase letters represent significant difference at p<0.05.

Fig.5 The firmness of fresh and thawed radish cylinders. (n=6); different lowercase letters represent significant difference at p<0.05.

Fig.6 Light micrographs of fresh and thawed radish tissue under the different processing conditions; (a) Fresh (b) SF (c) IF (d) UAF-1 (e) UAF-2 (f) UAF-3 (g) UAF-4, "DC" disruption of cells; "SC" separation of cells; Magnification: 200.

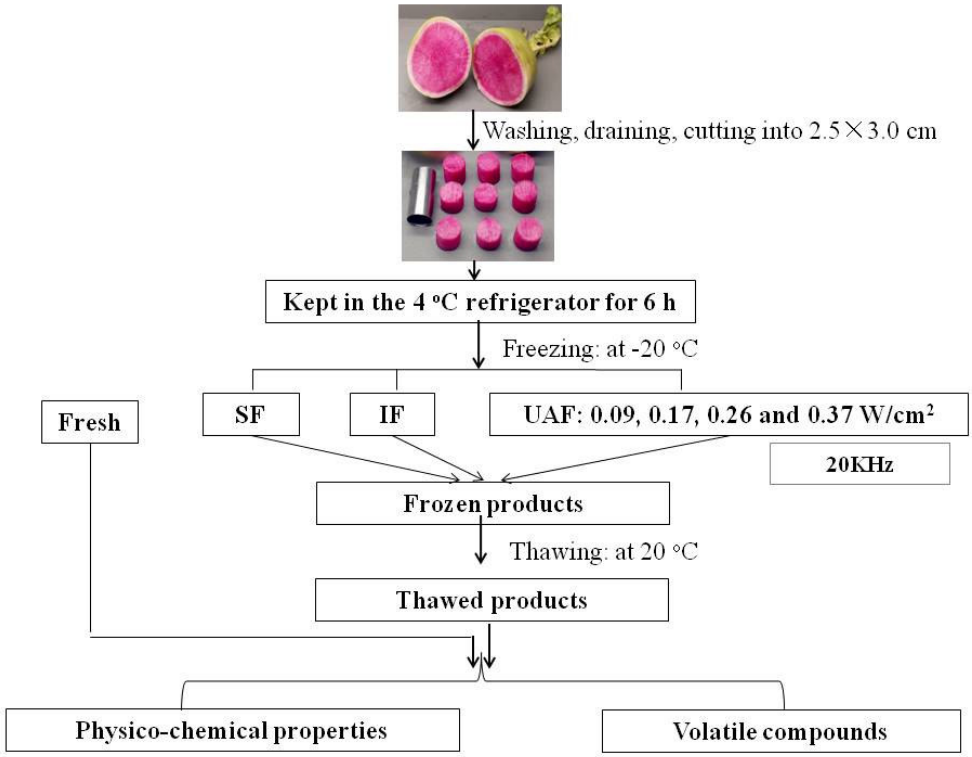

584

585 **Fig.1** Flowchart for experimental design; SF: slow freezing, IF: immersion freezing in

586 30% (w/v) $CaCl_2$, UAF: ultrasound-assisted freezing in 30% (w/v) $CaCl_2$.

587

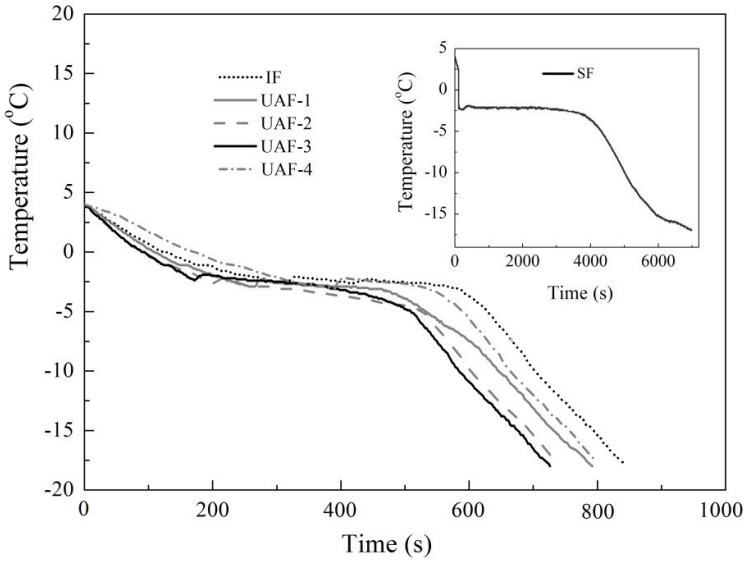

588

589 **Fig.2** The freezing curves of radish cylinders during the process of SF, IF and UAF at

590 different power intensities. (*n*=5).

591

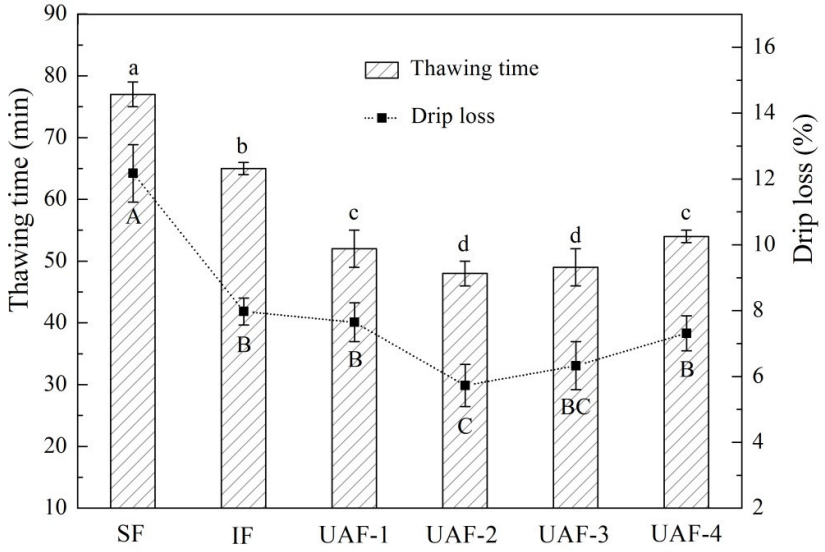

592

593 **Fig.3** The thawing time and drip loss of radish cylinders frozen by SF, IF, and UAF at

594 different power intensities. (n=3); different lowercase superscript letters (a–d)

595 represent significant differences of thawing time (p<0.05); different capital subscript

596 letters (A–D) represent significant differences of drip loss (p<0.05).

597

598

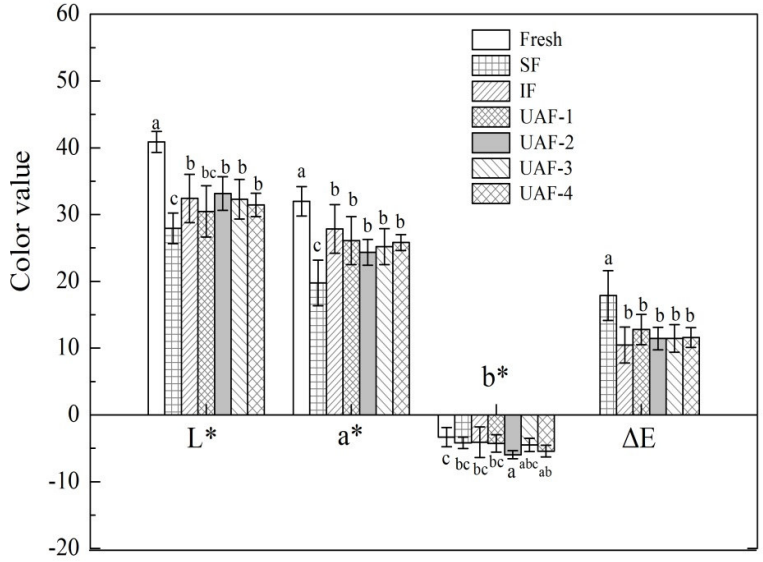

599 **Fig.4** The color of fresh and thawed radish cylinders. (n=6); different lowercase

600 letters represent significant difference at p<0.05.

601

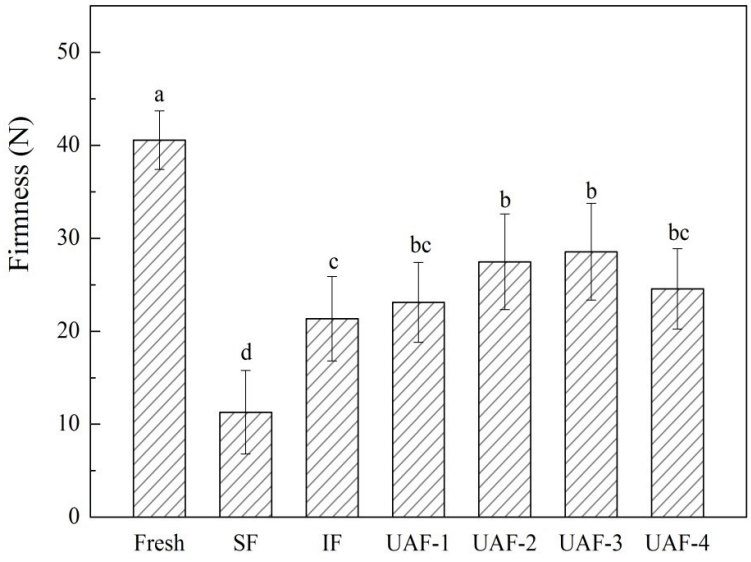

602

603 **Fig.5** The firmness of fresh and thawed radish cylinders. (n=6); different lowercase

604 letters represent significant difference at p<0.05.

605

606

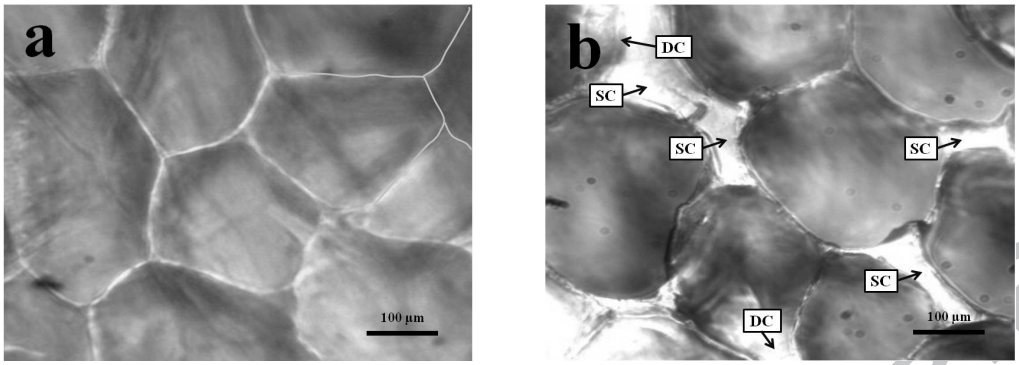

607

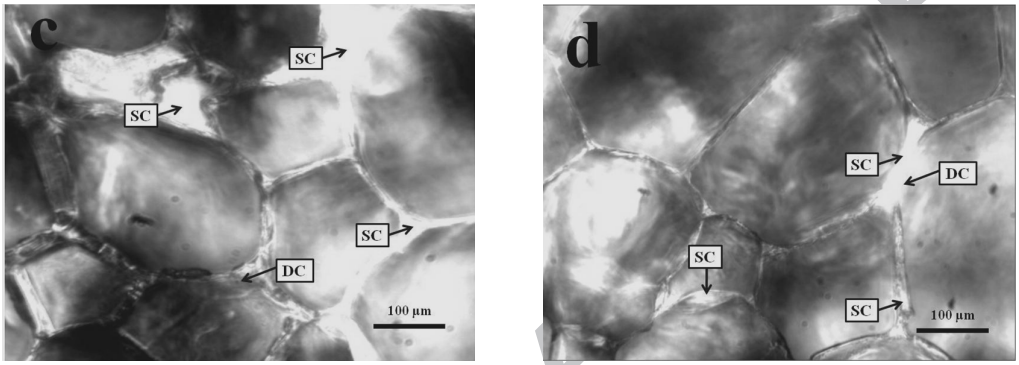

608

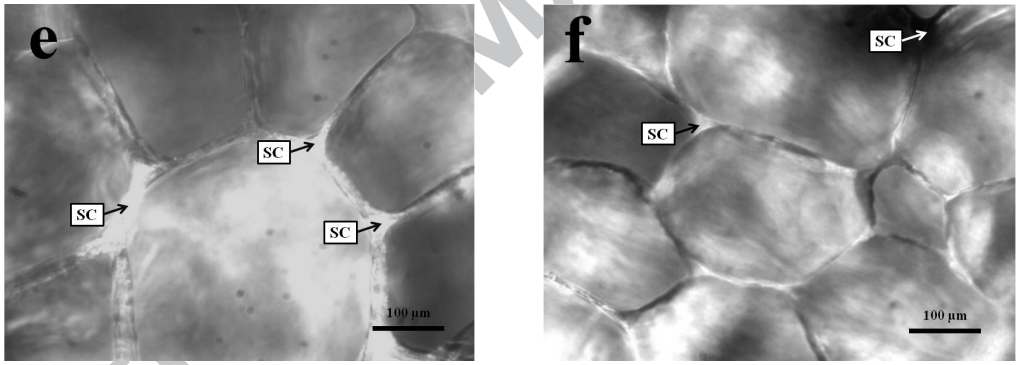

609

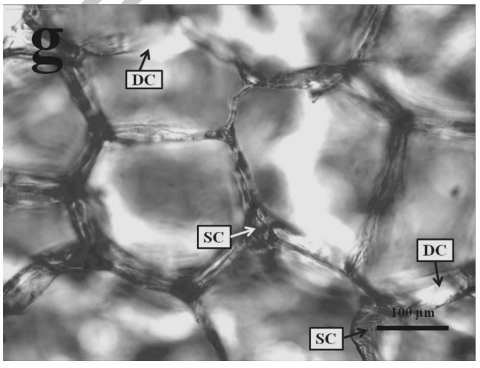

610 **Fig.6** Light micrographs of fresh and thawed radish tissue under the different

611 processing conditions; (a) Fresh (b) SF (c) IF (d) UAF-1 (e) UAF-2 (f) UAF-3 (g)

612 UAF-4 "DC" disruption of cells; "SC" separation of cells; Magnification: 400.

613 **Table 1** Total calcium content, total anthocyanin content, vitamin C (mg/100 g FW)
614 and total phenolics content (mg GAE/100 g FW) of thawed radish cylinders.(n=3)

Treatments	Total calcium content (mg/100 g)	Anthocyanin content (mg P3G/100 g)	Vitamin C content (mg/100 g)	Total phenolic content (mg GAE/100 g)
Fresh	57.20±2.61^{d}	63.81 ± 1.16^{a}	29.36 ± 0.86^{a}	88.13 ± 1.49^{a}
SF	48.55±3.35^{d}	48.44 ± 0.88^{d}	19.07 ± 1.98^{d}	71.21 ± 0.29^{d}
IF	514.44±5.32^{c}	52.55 ± 1.31^{c}	21.88 ± 1.71^{c}	75.02 ± 1.15^{c}
UAF-1	562.21±3.62^{b}	53.85 ± 2.11^{bc}	24.84 ± 1.52^{b}	80.98 ± 1.07^{b}
UAF-2	558.09±7.65^{b}	57.51 ± 0.76^{b}	25.73 ± 1.47^{b}	82.76 ± 0.64^{b}
UAF-3	549.48±3.85^{b}	56.93 ± 1.00^{b}	24.90 ± 0.91^{b}	83.06 ± 0.67^{b}
UAF-4	587.22±4.46^{a}	54.88 ± 1.63^{bc}	22.40 ± 1.12^{bc}	76.96 ± 0.78^{bc}

615 *Note:* P3G, pelargonidin-3-glucoside equivalents; GAE, gallic acid equivalents; Results are
616 mean ± standard deviation; values with different letters in the same column are significantly
617 different (p<0.05);

618

619 **Table 2** Volatile compounds and relative amount of fresh and thawed radish cylinders.

R.T./min	Compounds	Relative amount/%			
		Fresh	SF	IF	UAF-3
	Alcohols	**14.18**	**11.39**	**5.82**	**9.27**
1.97	Methanethiol	0.05	8.74	3.87	4.87
4.29	Ethanol	2.29	0.03	n.d.	n.d.
11.62	1-Pentanol	0.71	0.13	0.23	n.d.
13.91	1-Hexanol	4.41	n.d.	0.10	0.10
14.52	2-methyl-4-Penten-1-ol	0.19	n.d.	n.d.	0.83
15.69	1-octen-3-ol	n.d.	n.d.	0.25	0.42
15.69	1,3-Butanediol	1.72	n.d.	n.d.	0.24
15.80	1-Heptanol	0.83	0.20	0.10	0.42
17.24	Tetrahydro-2H-thiopyran-3-ol	n.d.	n.d.	0.01	0.02
17.39	1-Octanol	2.15	1.87	1.14	2.21
18.15	(E)-2-Octen-1-ol	0.42	0.08	0.03	n.d.
20.05	1-Decanol	0.11	0.04	n.d.	n.d.
22.31	1-Dodecanol	1.11	0.24	0.09	0.16
26.20	1-Hexadecanol	0.19	0.06	n.d.	n.d.
	Esters & Sulphurs	**49.37**	**62.67**	**78.18**	**72.65**
6.49	Ethanethioic acid, S-methyl ester	0.74	n.d.	n.d.	n.d.
7.02	Disulfide, dimethyl	2.63	7.50	3.49	1.29
11.72	1-isothiocyanato-Butane	0.87	0.32	0.12	0.23
11.881	Thiocyanic acid, methyl ester	n.d.	0.05	0.05	0.07
14.33	Trisulfide, dimethyl	1.36	n.d.	1.03	2.13
15.24	1-isothiocyanato-3-methyl-Butane	0.10	0.22	n.d.	n.d.
17.09	4-Methylpentyl isothiocyanate	2.00	2.22	1.48	1.82
17.83	1-isothiocyanato- Hexane	0.44	0.92	0.74	0.87
18.79	Carbonic acid, methyl octyl ester	n.d.	n.d.	0.22	0.31
22.57	3-(Methylthio) propyl isothiocyanate	3.13	2.04	2.83	2.45
24.09	4-isothiocyanato-1-(methylthio)-1-Butene	38.10	49.40	68.22	63.48
	Ketones	**3.72**	**2.19**	**1.46**	**1.78**
6.78	2,3-Pentanedione	0.10	n.d.	0.1	0.10
12.22	5-methyl- 2-Hexanone	0.12	n.d.	n.d.	0.12
12.69	1-hydroxy-2-Propanone	0.22	n.d.	n.d.	n.d.
13.46	6-methyl-5-hepten-2-one	0.13	0.04	0.04	0.02
16.79	3,5-Octadien-2-one	n.d.	n.d.	0.17	0.04
30.14	1-nitro-2-Octanone	3.15	2.15	1.15	1.50
	Aldehydes	**13.09**	**11.48**	**8.32**	**10.70**
7.26	Hexanal	2.87	1.50	1.79	1.99
9.69	Heptanal	0.34	0.61	0.43	0.58
12.27	Octanal	0.41	0.38	0.29	0.35
14.59	Nonanal	2.37	7.70	4.20	5.12
15.28	(E)-2-Octenal,	0.13	n.d.	0.24	0.15

15.85	2-Furancarboxaldehyde	1.95	0.17	n.d.	0.45
16.45	Decanal	1.16	0.40	0.48	0.95
16.84	Benzaldehyde	0.11	0.03	0.09	0.05
17.05	(E)-2-Nonenal	n.d.	n.d.	0.07	0.11
18.03	Undecanal	0.07	0.07	0.04	0.05
18.58	(Z)-2-Decenal	n.d.	n.d.	0.15	0.19
19.33	(E,E)-2,4-Undecadienal	n.d.	n.d.	0.13	0.23
19.42	Dodecanal	0.24	0.10	0.05	0.03
19.69	E-Citral	n.d.	0.03	0.01	0.02
19.95	E-2-dodecenal	n.d.	n.d.	0.08	0.03
20.69	Tridecanal	0.10	0.07	0.05	0.08
27.41	5-Hydroxymethylfurfural	3.34	0.42	0.22	0.32
Others		**8.75**	**2.97**	**3.10**	**1.04**
11.45	Bicyclo[4.2.0]octa-1,3,5-triene	2.36	n.d.	1.07	0.56
13.32	Dodecamethyl-cyclohexasiloxane,	1.25	n.d.	1.85	n.d.
16.22	Tetradecamethyl-cycloheptasiloxane,	4.44	2.83	n.d.	n.d.
21.02	Hexanoic acid	0.53	0.03	0.03	0.13
23.29	Octanoic acid	0.17	0.03	n.d.	n.d.
24.33	Nonanoic acid	n.d.	0.08	0.15	0.35

620 *Note:* n.d. not detected.
621
622
623
624
625

Effect of ultrasound-assisted freezing on the physico-chemical properties and volatile compounds of red radish

Bao-guo Xu[a], Min Zhang[a*], Bhesh Bhandari[b], Xin-feng Cheng[a] , Jincai Sun[c]

[a] State Key Laboratory of Food Science and Technology, Jiangnan University, 214122 Wuxi, Jiangsu, China

[b] School of Agriculture and Food Sciences, The University of Queensland, Brisbane, QLD 4072, Australia

[c]Haitong Food Group Company, Zhejiang Cixi, 315300, China

*Corresponding author: Professor Min Zhang, School of Food Science and Technology, Jiangnan University, 214122 Wuxi, Jiangsu Province, China.

E-mail: min@jiangnan.edu.cn Fax: 0086-(0)510-85807976

Highlights

- Ultrasound application can decrease freezing time and drip loss of red radish
- Ultrasound-assisted freezing (UAF) showed better retention on firmness and color
- UAF improved the retention of anthocyanins, vitamin C and phenolics content
- Microstructure of frozen radish was better preserved by UAF
- Red radish aromatic profile was deeply affected by the freezing/thawing process